AIMS Mathematics, 7(4): 6445–6466.
DOI: 10.3934/math.2022359
Received: 01 October 2021
Revised: 12 January 2022
Accepted: 17 January 2022
Published: 20 January 2022

http://www.aimspress.com/journal/Math

Research article

Dynamical analysis of an iterative method with memory on a family of third-degree polynomials

Beatriz Campos[1], Alicia Cordero[2], Juan R. Torregrosa[2,*] and Pura Vindel[1]

[1] Instituto de Matemáticas y Aplicaciones de Castellón, Universitat Jaume I, Castellón de la Plana, Spain

[2] Instituto de Matemática Multidisciplinar, Universitat Politècnica de València, València, Spain

* **Correspondence:** Email: jrtorre@mat.upv.es.

Abstract: Qualitative analysis of iterative methods with memory has been carried out a few years ago. Most of the papers published in this context analyze the behaviour of schemes on quadratic polynomials. In this paper, we accomplish a complete dynamical study of an iterative method with memory, the Kurchatov scheme, applied on a family of cubic polynomials. To reach this goal we transform the iterative scheme with memory into a discrete dynamical system defined on $\mathbf{R}^2$. We obtain a complete description of the dynamical planes for every value of parameter of the family considered. We also analyze the bifurcations that occur related with the number of fixed points. Finally, the dynamical results are summarized in a parameter line. As a conclusion, we obtain that this scheme is completely stable for cubic polynomials since the only attractors that appear for any value of the parameter, are the roots of the polynomial.

Keywords: nonlinear equation; Kurchatov's scheme; stability; dynamical plane; bifurcation; chaos; parameter line
Mathematics Subject Classification: 37N30, 37G35, 65H05

1. Introduction

Non-linearity is inherent in a wide variety of physical processes observed in real life, as well as in the systems underlying engineering problems. If they are linearized for the sake of greater simplicity, then much of the complexity disappears, but it is also removed from the reality that defines it and, therefore, the solution to the problem is a worse approximation of the real solution. Iterative schemes are very useful in this context in order to estimate the solution of nonlinear equations, $f(x) = 0$, that model these kind of problems.

Although the most known fixed-point iterative method is Newton's scheme, it is only the reference

for a subclass of numerical procedures: iterative schemes without memory, due to the fact that it only uses the actual iterate in order to calculate the next one of the sequence that will converge to the solution. There exists another class of iterative schemes that use more than one known iterate to calculate the following one: they are known as iterative procedures with memory, and the most known scheme with memory is the classical secant one, whose iterative expression is

$$x_{n+1} = x_n - \frac{f(x_n)(x_n - x_{n-1})}{f(x_n) - f(x_{n-1})},\ n = 1, 2, \ldots$$

being x_0 and x_1 initial guesses. The simplicity of its expression makes it very useful but its convergence is only super-linear, in contrast with the quadratic convergence of Newton's scheme. To overload this inconvenient, Kurchatov designed in [1], by using interpolation techniques, the root-finding algorithm known as Kurchatov's scheme,

$$\begin{aligned} \Delta_n &= x_n - x_{n-1}, \\ x_{n+1} &= x_n - \frac{2f(x_n)\Delta_n}{f(x_n + \Delta_n) - f(x_n - \Delta_n)}, \end{aligned}$$

that is also an iterative method with memory that holds the second order of convergence of Newton's scheme.

In the last years, different schemes with memory have been designed (a good overview can be found in [2]) with increasing order of convergence (and, therefore, higher computational complexity). In terms of stability, some researchers compared the wideness of their basins of attraction (the set of starting points converging to the same attractor) by using techniques of discrete dynamics. In [3], the authors observed that iterative schemes with memory of seventh-order of convergence showed better stability properties than many optimal eight-order procedures without memory. This graphical comparison was used afterwards by different authors; see, for example, the work by Cordero et al. [4], that of Wang et al. [5] in 2016 or the research by Bakhtiari et al. in [6] and Howk et al. [7] in the following years.

Meanwhile, the authors developed in [8] a technique using multidimensional real discrete dynamics, able to analyze the stability of iterative schemes with memory, not only in graphical terms, but essentially analytical. It has also been used to make a brief analytical study of other schemes as in the paper by the authors [9], or that defined by Choubey et al. in [10], or those by Chicharro et al. in [11–13].

A key fact to deeply understand the performance of the iterative schemes are the poles of the rational functions composing its multidimensional operator.

If we denote by $x_{n-1} = x$ and $x_n = y$, as it was defined in [8, 9], the algorithm of Kurchatov can be studied from a dynamical point of view as a two dimensional map

$$K : \begin{pmatrix} x \\ y \end{pmatrix} \to \begin{pmatrix} y \\ y - \frac{2f(y)(y-x)}{f(2y-x)-f(x)} \end{pmatrix}, \tag{1.1}$$

with a vanishing denominator.

In [14], a parametric family of iterative procedures, including Kurchatov's scheme, was designed. By using the tools of multidimensional real discrete dynamics, the performance on quadratic polynomials is studied pointing out many particular schemes with very good properties in terms of stability

and wideness of the set of converging starting points; several other methods found with unstable or even chaotic performance were also described as members of this class of iterative procedures.

As far as we know, there are not many papers dealing with the dynamics of iterative methods with memory applied on polynomials of degree greater than two. A complete study of the secant method for polynomials of arbitrary degree can be found in [20, 21]. In [22], Bairstow's method is studied for a family of cubic polynomials equivalent to the one studied in this paper.

Our goal in this manuscript is to analyze the behaviour of Kurchatov's method on cubic polynomials and state its stability in this context. To get this aim, we introduce in the following section some concepts and properties of multidimensional real discrete dynamics that are used in the subsequent sections. Our final conclusion is that this scheme is stable for every value of the parameter of the family these polynomials.

The rest of this manuscript is organized as follows: Section 2 is devoted to introduce all these necessary concepts and tools for the analysis of the stability of the fixed points of the multidimensional rational operator associated to Kurchatov's scheme on a generic cubic polynomial $p(x) = x(x-1)(x-a)$ in Section 3. We also analyze the focal points and prefocal lines, that help us to delimit the boundaries of the basins of attraction. In Section 3.2, we study the inverses of the mentioned rational operator and their properties. The basins of attraction of the fixed points of the rational operator are presented, and the dynamical planes and bifurcations are also studied. The manuscript finishes with the conclusions and the references used.

2. Materials and methods

In this section we recall some basic concepts related with multidimensional dynamics. Let us denote as T a vectorial rational operator. We define the *orbit* of $x^{(0)}$ as a set of the successive images by T, that is, $\{x^{(0)}, T(x^{(0)}), \ldots, T^m(x^{(0)}), \ldots\}$. Indeed, the dynamical behavior of a point $x \in \mathbf{R}^n$ can be characterized by analyzing its asymptotic performance, thus x^* such that $T(x^*) = x^*$ is called a *fixed point of* T. Some results about stability of fixed points are summarized in the next result ([15]).

Theorem 2.1. *Let $T : \mathbf{R}^n \to \mathbf{R}^n$ be C^2. Assume x^* is a fixed point. Let $\lambda_1, \lambda_2, \ldots, \lambda_n$ be the eigenvalues of the Jacobian $JT(x^*)$. Then,*

a) If $|\lambda_j| < 1$, $\forall j \in \{1, 2, \ldots, n\}$, then x^* is attracting.
b) If, at least, one eigenvalue λ_{j0} holds $|\lambda_{j0}| > 1$, then x^* is unstable, that is, repelling or saddle.
c) If $|\lambda_j| > 1$, $\forall j \in \{1, 2, \ldots, n\}$, then x^* is repelling.

Indeed, if x^* is an attracting fixed point of the rational function T, we define its *basin of attraction* $\mathcal{A}(x^*)$ as the set of preimages of any order such that

$$\mathcal{A}(x^*) = \{x^{(0)} \in \mathbf{R}^n : T^m(x^{(0)}) \to x^*, m \to \infty\}$$

and it is denoted by $\mathcal{A}^*(x^*)$ if the set of preimages considered is in the same connected component as x^*.

Now, we recall some definitions and properties related to maps with vanishing denominators. We refer to [16–19, 24, 25] for a more complete study.

Definition 2.2. A *map with vanishing denominator* is a map T of $\mathbf{R}^n$, with $n \geq 2$, that is not defined in the whole space $\mathbf{R}^n$ because at least one of its components contains a denominator that can vanish. The set of points δ_T where the denominators vanish is called the *set of non definition* of the map.

We consider an arbitrary map of the form:

$$T : \begin{pmatrix} x \\ y \end{pmatrix} \to \begin{pmatrix} F(x,y) \\ G(x,y) = \frac{N(x,y)}{D(x,y)} \end{pmatrix}, \tag{2.1}$$

where the continuously differentiable functions $F(x,y), N(x,y)$ and $D(x,y)$ have not common factors and are defined on the whole plane $\mathbf{R}^2$. The *set of non definition*

$$\delta_T = \{(x,y) \in \mathbf{R}^2 / D(x,y) = 0\}$$

is usually made of the union of smooth curves in the plane.

Many global properties of two dimensional maps can be explained from the analysis of some kinds of singularities, such as the sets where the denominator of the map vanishes, some inverses vanish, their preimages and the points where the map takes the form $0/0$.

2.1. Focal points and prefocal lines

As commented before, some dynamical properties of two-dimensional maps can be explained from the analysis of their singularities, such as the set of points where the denominator of the map (or some of its inverses) vanishes, see [19, 23]. The following definition helps us to understand it.

Definition 2.3. Consider a two dimensional map T of the form (2.1). A point Q that belongs to the set of non-definition δ_T, is a *focal point* if at least one component of the map takes the form $0/0$ in Q and there exist smooth simple arcs $\gamma(\tau)$ with $\gamma(0) = Q$, such that $\lim_{\tau\to 0} T(\gamma(\tau))$ is finite. The set of all such finite values, obtained by taking different arcs $\gamma(\tau)$ through Q, is called the *prefocal set* δ_Q.

A focal point Q is *simple* if:

$$(N_x D_y - N_y D_x)|_Q \neq 0.$$

Let us consider a smooth simple arc γ transverse to δ_T (not tangential) and look how it is transformed by applying the map T, that is, what is the shape of its image. Consider a point $(x_0, y_0) \in \delta_T$ and assume that in a neighborhood of (x_0, y_0) the arc γ is represented by the parametric equations:

$$\gamma(\tau) = \begin{cases} x(\tau) = x_0 + \xi_1\tau + \xi_2\tau^2 + \cdots \\ y(\tau) = y_0 + \eta_1\tau + \eta_2\tau^2 + \cdots \end{cases}$$

with $\tau \neq 0$. As $(x_0, y_0) \in \delta_T$, there exists a vanishing denominator, but if the numerator is different from zero, then:

$$\lim_{\tau\to 0} T(\gamma(\tau)) = (y_0, \infty).$$

This means that the image $T(\gamma(\tau))$ is made up of two disjoint arcs asymptotic to the line $x = y_0$. Different arcs through the same point are mapped into different arcs asymptotic to the same line, see Figure 1.

If the point $(x_0, y_0) \in \delta_T$ satisfies that both numerator and denominator vanish, then the limit can be finite and the image of an arc can be bounded, see Figure 2.

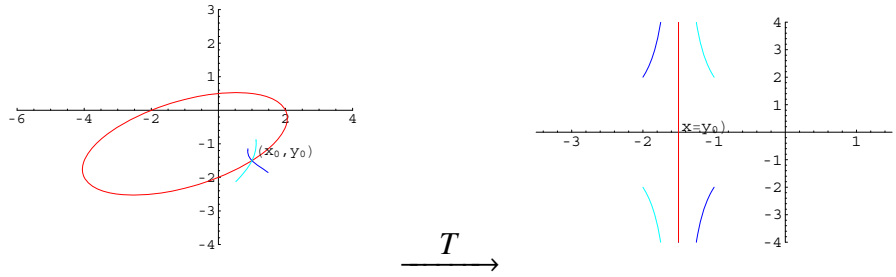

Figure 1. Mapping T_a on transverse arcs with unbounded image.

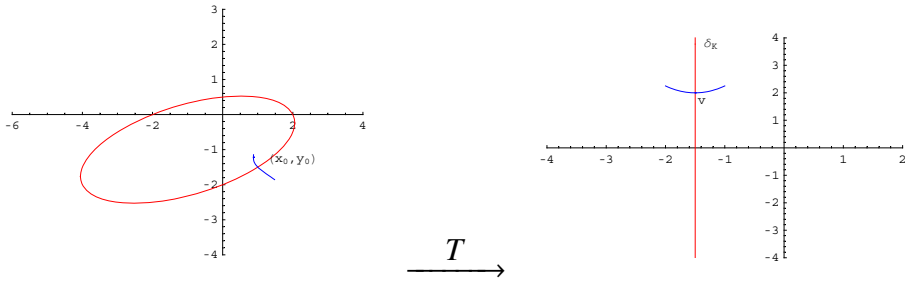

Figure 2. Mapping T_a on transverse arcs with bounded image.

3. Results and discussion

3.1. Kurchatov's method applied on cubic polynomials

In this paper, we study the dynamics of the map K associated to the Kurchatov's method given in (1.1), when $f(x)$ is a generic cubic polynomial, $p(x) = x(x-1)(x-a)$ and a is real. By applying (1.1) to this polynomial, we obtain a uniparametric family of maps:

$$K_a : \begin{pmatrix} x \\ y \end{pmatrix} \to \begin{pmatrix} y \\ \frac{y(x^2+3y^2-y(1+a+2x))}{x^2+4y^2-2y(1+a+x)+a} \end{pmatrix}. \tag{3.1}$$

The set of non definition of K_a is given by the ellipse

$$\delta_{K_a} = \{(x, y) \in \mathbf{R}^2 / x^2 + 4y^2 - 2y(1 + a + x) + a = 0\}.$$

So, the iteration of K_a is well defined, provided that the initial condition belongs to the set E given by:

$$E = \mathbf{R}^2 \backslash \Lambda,$$

where

$$\Lambda = \bigcup_{n \geq 0} K_a^{-n}(\delta_{K_a}),$$

that is, Λ is the set of preimages (of any order) of the ellipse δ_{K_a} cancelling the denominator of a component of the rational operator.

The iterations of the map $K_a : E \to E$ can be considered as a discrete dynamical system. As the singular set δ_{K_a} corresponds to a curve in the plane, the set of points excluded from the phase space of the iterations of K_a has zero Lebesgue mesure in $\mathbf{R}^2$.

3.1.1. Fixed points of K_a

Proposition 3.1. *The fixed points of map K_a are $(0,0)$, $(1,1)$ and (a,a) and all of them are attractive.*

Proof. The fixed points satisfy $K_a(x_0, y_0) = (x_0, y_0)$. In this case, the fixed points coincide with the roots of the cubic polynomial:

$$K_a\begin{pmatrix} x \\ y \end{pmatrix} = \begin{pmatrix} x \\ y \end{pmatrix} \Rightarrow \begin{pmatrix} y \\ \frac{y(x^2+3y^2-y(1+a+2x))}{x^2+4y^2-2y(1+a+x)+a} \end{pmatrix} = \begin{pmatrix} x \\ y \end{pmatrix}.$$

From the first equation we obtain $x = y$. The second equation gives:

$$y(x^2 + 3y^2 - y(1 + a + 2x)) = y(x^2 + 4y^2 - 2y(1 + a + x) + a).$$

One solution is $y = 0$. For $y \neq 0$, $x^2 + 3y^2 - y(1 + a + 2x) = x^2 + 4y^2 - 2y(1 + a + x) + a$. By substituting $y = x$ and simplifying:

$$y^2 - y(1 + a) + a = 0 \quad \Rightarrow \quad y = 1, y = a.$$

Then, the fixed points coincide with the roots of the cubic polynomial.

In order to study their stability we build the Jacobian matrix:

$$JK_a(x, y) = \begin{pmatrix} 0 & 1 \\ \frac{\partial G}{\partial x} & \frac{\partial G}{\partial y} \end{pmatrix}$$

where:

$$\begin{aligned} \frac{\partial G}{\partial x} &= \frac{-2y(y-1)(y-a)(y-x)}{(x^2 + 4y^2 - 2y(1 + a + x) + a)^2}, \\ \frac{\partial G}{\partial y} &= \frac{x^2(a + x^2) - 2(1 + a + 2x)(a + x^2)y + (2(1 + a)^2 + 6x(1 + a) + 9(a + x^2))y^2}{(x^2 + 4y^2 - 2y(1 + a + x) + a)^2} + \\ &+ \frac{-12(1 + a + x)y^3 + 12y^4}{(x^2 + 4y^2 - 2y(1 + a + x) + a)^2}. \end{aligned}$$

Then, the fixed points are attractive since the value of the Jacobian evaluated at each of them is:

$$JK_a(x, y) = \begin{pmatrix} 0 & 1 \\ 0 & 0 \end{pmatrix}.$$

□

The following property gives us the lines on the plane that are mapped onto the fixed points.

Property 3.2. Let $R = (x^*, y^*)$ be a fixed point of K_a. Then, $K_a(x, y) = (x^*, y^*)$ if and only if $y = y^*$.

Proof. The fixed points of K_a are $(0,0)$, $(1,1)$ and (a,a).

For $R = (0,0)$

$$K_a(x,y) = (0,0) \Leftrightarrow \begin{pmatrix} y \\ \frac{y(x^2+3y^2-y(1+a+2x))}{x^2+4y^2-2y(1+a+x)+a} \end{pmatrix} = \begin{pmatrix} 0 \\ 0 \end{pmatrix} \Leftrightarrow y = 0.$$

Similarly, for $R = (1,1)$

$$K_a(x,y) = (1,1) \Leftrightarrow y = 1$$

and for $R = (a,a)$

$$K_a(x,y) = (a,a) \Leftrightarrow y = a.$$

That is, the line $y = y^*$ is mapped onto the fixed point R. □

3.1.2. Focal points and prefocal curves of K_a

Focal points are defined as those points where at least one of the components of the two dimensional map is $0/0$ with finite limit. In our case, we obtain two simple focal points for almost all values of a.

Now, let us consider the two dimensional map K_a defined by (3.1).

Proposition 3.3. *The map K_a has two simple focal points Q_1 and Q_2 with associated prefocal sets δ_{Q_1} and δ_{Q_2} respectively, given by:*

- $Q_1 = \left(-\sqrt{-a}, 0\right)$, $Q_2 = \left(\sqrt{-a}, 0\right)$,
  $\delta_{Q_1} = \delta_{Q_2} = \{(x,y) \in \mathbf{R}^2 / x = 0\}$ *for* $a < 0$.

- $Q_1 = \left(a - \sqrt{a(1-a)}, a\right)$, $Q_2 = \left(a + \sqrt{a(1-a)}, a\right)$,
  $\delta_{Q_1} = \delta_{Q_2} = \{(x,y) \in \mathbf{R}^2 / x = a\}$ *for* $0 < a < 1$.

- $Q_1 = \left(1 - \sqrt{a-1}, 1\right)$, $Q_2 = \left(1 + \sqrt{a-1}, 1\right)$,
  $\delta_{Q_1} = \delta_{Q_2} = \{(x,y) \in \mathbf{R}^2 / x = 1\}$ *for* $a > 1$.

For $a = 0$ and $a = 1$, the focal points are double and coincide with the double root of the polynomial.

Proof. Focal points of K_a satisfy the equations:

$$\begin{aligned} y(x^2 + 3y^2 - y(1 + a + 2x)) &= 0, \\ x^2 + 4y^2 - 2y(1 + a + x) + a &= 0. \end{aligned}$$

The first equation implies $y = 0$ or $x^2 + 3y^2 - y(1 + a + 2x) = 0$. Taking $y = 0$ and substituting in the second equation, we obtain $x^2 + a = 0$; so, the points $\left(-\sqrt{-a}, 0\right)$ and $\left(\sqrt{-a}, 0\right)$ are obtained, that exist for $a \leq 0$.

From $x^2 + 3y^2 - y(1 + a + 2x) = 0$ we can deduce $x^2 - 2yx = -3y^2 + y(1 + a)$, and substituting in the second equation we obtain:

$$-3y^2 + y(1 + a) + 4y^2 - 2y(1 + a) + a = 0 \Rightarrow y^2 - y(1 + a) + a = 0 \Rightarrow y = 1 \text{ or } y = a.$$

If $y = 1$, then $x^2 - 2x = -2 + a \Rightarrow x = 1 \pm \sqrt{a-1}$, that exists if $a > 1$. For $y = a$, then $x^2 - 2ax = -2a^2 + a \Rightarrow x = a \pm \sqrt{a(1-a)}$, that exists if $0 \leq a \leq 1$. It is easy to check that when $a = 0$ there is a unique focal point at $(0, 0)$, that is also a double root of the polynomial; for $a = 1$, the double focal point is $(1, 1)$.

As said above, for a map T as given by (2.1), a focal point Q is *simple* if:

$$(N_x D_y - N_y D_x)|_Q \neq 0.$$

In our case:

$$\begin{aligned} N(x,y) &= y(x^2 + 3y^2 - y(1 + a + 2x)), \\ D(x,y) &= x^2 + 4y^2 - 2y(1 + a + x) + a. \end{aligned}$$

It can be checked that:

$$\begin{aligned} (N_x D_y - N_y D_x)|_{Q_{1,2}} &= \pm 2a\sqrt{-a}, \quad a < 0, \\ (N_x D_y - N_y D_x)|_{Q_{1,2}} &= \mp 2a(1-a)\sqrt{a(1-a)}, \quad 0 < a < 1, \\ (N_x D_y - N_y D_x)|_{Q_{1,2}} &= \mp 2(a-1)\sqrt{a-1}, \quad a > 1. \end{aligned}$$

Then, the focal points are simple for any value of the parameter different from $a = 0$ and $a = 1$. On the other hand, for $a = 0$ and for $a = 1$ focal points coincide with the double root of the polynomial and they are not simple.

Let us obtain the prefocal sets. For a given value a, $a \neq 0$ and $a \neq 1$, consider a focal point $Q = (x_0, y_0) \in \delta_{K_a}$, and take smooth simple arcs γ transverse to δ_{K_a} at this point, represented by the parametric equations:

$$\gamma(\tau) = \begin{cases} x(\tau) = x_0 + \xi_1 \tau + \xi_2 \tau^2 + ... \\ y(\tau) = y_0 + \eta_1 \tau + \eta_2 \tau^2 + ... \end{cases}$$

with $\tau \neq 0$. Then, if we apply the map K_a on this point the numerator and the denominator vanish and

$$\lim_{\tau \to 0} K_a(\gamma(\tau)) = \left(y_0, \lim_{\tau \to 0} \frac{N(\gamma(\tau))}{D(\gamma(\tau))} \right) = (x_\gamma, y_\gamma).$$

Then, $x_\gamma = y_0$ and

$$y_\gamma = \frac{\overline{N_x} + \overline{N_y} m}{\overline{D_x} + \overline{D_y} m},$$

where $m = \dfrac{\xi_1}{\eta_1}$ and $\overline{N_x}$ means the derivative of N respect to x evaluated in the focal point.

For $a < 0$, the focal points are $Q_1 = \left(-\sqrt{-a}, 0 \right), Q_2 = \left(\sqrt{-a}, 0 \right) \in \delta_{K_a}$. Then, $x_\gamma = 0$ and

$$y_\gamma = \frac{am}{2\left(\pm\sqrt{-a} + \left(1 + a \pm \sqrt{-a} \right) m \right)}.$$

Let us notice that the values of y_γ go over the entire real line except when $m = \frac{\pm\sqrt{-a}}{1+a\pm\sqrt{-a}}$. This value of the slope corresponds to curves that are tangent to δ_{K_a} at the focal points.

The same can be proven for the focal points obtained for the other values of a. So, the prefocal sets in our case are given by $x = F(Q)$ (see [16]):

$$\begin{aligned} x &= 0, \ a < 0, \\ x &= a, \ 0 < a < 1, \\ x &= 1, \ a > 1, \end{aligned}$$

where $F : \mathbf{R}^2 \to \mathbf{R}^2$ is defined in (3.1). □

3.2. Inverses of K_a and their properties

In order to understand the global dynamical properties of a map, it is important to see how many inverses map has K_a and in which regions of the phase plane the inverses are defined. Let (x', y') be a given point of the plane. Then, by solving the system of equations obtained from (3.1), we can get either two distinct real solutions, called rank-1 preimages of point (x', y'), or no real solutions. We call Z_2 and Z_0 the regions of the plane whose points have, respectively, two distinct rank-1 preimages and no preimages at all.

$$K_a^{-1} : \begin{pmatrix} x' \\ y' \end{pmatrix} \to \begin{pmatrix} x = x' \pm \sqrt{\Delta} \\ y = x' \end{pmatrix}, \tag{3.2}$$

where

$$\Delta = \frac{-2x'^3 + ay' - 2(1+a)x'y' + x'^2(1+a+3y')}{x' - y'}.$$

These regions are given by:

$$\begin{aligned} Z_0 &= \{(x,y) \in \mathbf{R}^2 \,/\, -2x^3 + ay - 2(1+a)xy + x^2(1+a+3y) > 0, x - y < 0\} \\ &\bigcup \{(x,y) \in \mathbf{R}^2 \,/\, -2x^3 + ay - 2(1+a)xy + x^2(1+a+3y) < 0, x - y > 0\}, \\ Z_2 &= \{(x,y) \in \mathbf{R}^2 \,/\, -2x^3 + ay - 2(1+a)xy + x^2(1+a+3y) > 0, x - y > 0\} \\ &\bigcup \{(x,y) \in \mathbf{R}^2 \,/\, -2x^3 + ay - 2(1+a)xy + x^2(1+a+3y) < 0, x - y < 0\}, \end{aligned}$$

and they are separated by the line $y = x$ and the graphic of the rational function $y = \frac{x^2(2x-(a+1))}{3x^2-2(a+1)x+a}$. These curves form the boundary of the regions Z_0 and Z_2, but they are not a locus of critical points where the two inverses are defined and merge, since the denominator vanishes for $y = x$.

Let

$$LC = \left\{(x,y) \in \mathbf{R}^2 / y = f(x) = \frac{x^2(2x-(a+1))}{3x^2 - 2(a+1)x + a}\right\} \tag{3.3}$$

be the *critical set*, that is, the set of points where the preimages merge.

Merging preimages are located in another set of points LC_{-1} that is included in the set of points in which the determinant of the Jacobian matrix vanishes:

$$LC_{-1} \subset J_0 = \{(x,y) \in \mathbf{R}^2 / \det J(K_a) = 0\}.$$

Moreover, it is easy to check the following results.

Property 3.4. The intersection of the two curves that form the boundary of Z_0 and Z_2 are the fixed points.

Proof. The solutions of the system

$$\begin{aligned} y &= \frac{x^2(2x-(a+1))}{3x^2-2(a+1)x+a}, \\ y &= x, \end{aligned}$$

are $(0,0)$, $(1,1)$ and (a,a). □

Property 3.5. The inverse of the curve LC is given by

$$LC_{-1} = \{(x,y) \in \mathbf{R}^2 / y = x\}.$$

Moreover, $LC_{-1} \subset J_0$.

Proof. It is easy to check that

$$K_a(x,x) = \left(x, \frac{x^2(2x-(a+1))}{3x^2-2(a+1)x+a}\right).$$

As $J_0 = \{(x,y) \in \mathbf{R}^2 / \det J(K_a) = 0\}$ and $\det J(K_a) = \frac{2y(y-1)(y-a)(y-x)}{(x^2+4y^2-2y(1+a+x)+a)^2}$, then $LC_{-1} \subset J_0$. □

Property 3.6. The fixed points are critical points of LC.

Proof. The derivative of $f(x) = \frac{x^2(2x-(a+1))}{3x^2-2(a+1)x+a}$ is $f'(x) = \frac{2x(x-1)(x-a)(3x-(a+1))}{(3x^2-2(a+1)x+a)^2}$.

So, $f'(x)$ vanishes for $x = 0$, $x = 1$ and $x = a$, that coincide with the fixed points. □

Property 3.7. The points of intersection of the set δ_{K_a} and the line $y = x$ belong to the asymptotes of LC. Moreover, they are the maximum and the minimum of the ellipse δ_{K_a}.

Proof. It is easy to check that the points satisfying the equations:

$$\begin{aligned} 4y^2 + x^2 - 2y(1+a+x) + a &= 0, \\ x &= y, \end{aligned}$$

are:

$$\begin{aligned} P_1 &= \left(\frac{1+a-\sqrt{a^2-a+1}}{3}, \frac{1+a-\sqrt{a^2-a+1}}{3}\right), \\ P_2 &= \left(\frac{1+a+\sqrt{a^2-a+1}}{3}, \frac{1+a+\sqrt{a^2-a+1}}{3}\right), \end{aligned}$$

so, they belong to the asymptotes of LC. On the other hand, the slope of the tangent lines to the ellipse is $y'|_P = \frac{y-x}{4y-(1+a+x)}\Big|_P$; this slope vanishes if the point satisfies $x = y$, being $y'' \neq 0$. □

3.3. Basins of attraction of the map

In this section, we describe the basins of attraction of the fixed points and their bifurcations as the parameter a varies. As we have said before, this map has three fixed points for every value of the parameter except for $a = 0$ and $a = 1$, where two of the fixed points collide. Moreover, for these values the two focal points also collide and coincide with the double fixed point.

Another bifurcation occurs when the focal points are in Z_2 and change to be in Z_0. This kind of bifurcation is described in the next result.

Lemma 3.8. *Focal points Q_1 and Q_2 satisfy the following statements:*

- *Q_1 has two preimages if and only if $a \in (-\infty, -3 - 2\sqrt{2}) \cup (\frac{1}{4}(2 + \sqrt{2}), 2(2 - \sqrt{2}))$.*
- *Q_1 has one preimage if and only if $a = -3 - 2\sqrt{2}$ or $a = \frac{1}{4}(2 + \sqrt{2})$ or $a = 2(2 - \sqrt{2})$.*
- *Q_1 has no preimage for the other parameter values.*
- *Q_2 has two preimages if and only if $a \in (-3 + 2\sqrt{2}, \frac{1}{4}(2 - \sqrt{2})) \cup (2(2 + \sqrt{2}), \infty)$.*
- *Q_2 has one preimage if and only if $a = -3 + 2\sqrt{2}$ or $a = \frac{1}{4}(2 - \sqrt{2})$ or $a = 2(2 + \sqrt{2})$.*
- *Q_2 has no preimage for the other parameter values.*

Proof. For $a < 0$, the preimages of $Q_1 = (-\sqrt{-a}, 0)$ satisfy the system:

$$\begin{aligned} y &= -\sqrt{-a}, \\ x^2 + 3y^2 - y(1 + a + 2x) &= 0, \end{aligned}$$

whose solution is

$$x = -\sqrt{-a} \pm \sqrt{-\sqrt{-a}(a + 1) + 2a}.$$

The values of the parameter that satisfy $-\sqrt{-a}(a + 1) + 2a > 0$ and $a < 0$ are those satisfying $a < -3 - 2\sqrt{2}$. For $a = -3 - 2\sqrt{2}$, then Q_1 has one preimage.

Following the same reasoning it is easy to check that the focal point $Q_2 = (\sqrt{-a}, 0)$ has two preimages if $\sqrt{-a}(a + 1) + 2a > 0$ and $a < 0$, that implies $-3 + 2\sqrt{2} < a < 0$. For $a = -3 + 2\sqrt{2}$, then Q_2 has one preimage.

For $0 < a < 1$, the preimages of $Q_1 = (a - \sqrt{a(1 - a)}, a)$ satisfy:

$$\begin{aligned} y &= a - \sqrt{a(1 - a}, \\ \frac{x^2 + 3y^2 - y(1 + a + 2x)}{x^2 + 4y^2 - 2y(1 + a + x) + a} &= a, \end{aligned}$$

whose solution is

$$x = a - \sqrt{a(1 - a)} \pm \sqrt{2a(a - 1) + (2a - 1)\sqrt{a(1 - a)}}.$$

The values of the parameter that satisfy $2a(a - 1) + (2a - 1)\sqrt{a(1 - a)} > 0$ and $0 < a < 1$ are those verifying $\frac{1}{4}(2 + \sqrt{2}) < a < 1$. For $a = \frac{1}{4}(2 + \sqrt{2})$, then Q_1 has one preimage.

With the same reasoning it is easy to check that the focal point $Q_2 = (a + \sqrt{a(1 - a)}, a)$ has two preimages if $0 < a < \frac{1}{4}(2 - \sqrt{2})$. For $a = \frac{1}{4}(2 - \sqrt{2})$, Q_2 has one preimage.

Finally, for $a > 1$, the preimages of $Q_1 = (1 - \sqrt{a - 1}, 1)$ satisfy:

$$y = 1 - \sqrt{a - 1},$$

$$\frac{x^2+3y^2-y(1+a+2x)}{x^2+4y^2-2y(1+a+x)+a} = 1,$$

whose solution is

$$x = 1-\sqrt{a-1} \pm \sqrt{2(1-a)+(2-a)\sqrt{a-1}}.$$

The values of the parameter that satisfy $2(1-a)+(2-a)\sqrt{a-1} > 0$ and $a > 1$ are those satisfying $1 < a < 2(2-\sqrt{2})$. For $a = 2(2-\sqrt{2})$, then Q_1 has one preimage.

Similarly, it is easy to check that the focal point $Q_2 = (1+\sqrt{a-1}, 1)$ has two preimages if $a > 2(2+\sqrt{2})$. For $a = 2(2+\sqrt{2})$, then Q_2 has one preimage. □

Remark 3.9. Let us notice that the focal points have not any preimage if $a \in (-3-2\sqrt{2}, -3+2\sqrt{2}) \cup (\frac{1}{4}(2-\sqrt{2}), \frac{1}{4}(2+\sqrt{2})) \cup (2(2-\sqrt{2}), 2(2+\sqrt{2}))$.

Remark 3.10. There is not any parameter value for which both focal points have preimages simultaneously.

These results can be observed in Figure 3, where focal points are colored in blue.

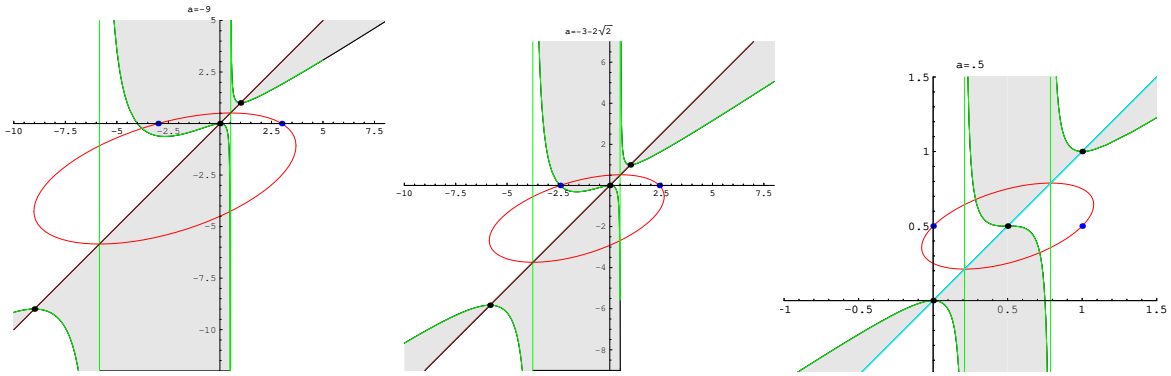

Figure 3. Location of the focal points for different values of a.

In Figure 3 we can also observe that there is always a fixed point surrounded by the singular set δ_{K_a}, which leads to the next result:

Proposition 3.11. *Let $R_i = (x_i^*, x_i^*), i = 1, 2, 3$, be the three fixed points such that $x_1^* < x_2^* < x_3^*$. Then, the immediate basin of attraction of R_2 is bounded.*

Proof. For $a < 0$, the three fixed points are $R_1 = (a, a)$, $R_2 = (0, 0)$ and $R_3 = (1, 1)$. By substituting the point $(0, 0)$ in the equation of δ_{K_a} we obtain a, as $a < 0$ we have that $R_2 = (0, 0)$ is located in the interior of the closed curve of δ_{K_a}. On the other hand, by substituting R_1 and R_3 we obtain $a^2+4a^2-2a(1+a+a)+a = a^2-a = a(a-1) > 0$ and $1+4-2(1+a+1)+a = 1-a > 0$, respectively, that means that $R_1 = (a, a)$ and $R_3 = (1, 1)$ are located in the exterior of δ_{K_a}.

For $0 < a < 1$, then $R_2 = (a, a)$. By substituting it in equation δ_{K_a} we obtain $a^2 + 4a^2 - 2a(1 + a + a) + a = a^2 - a = a(a-1) < 0$. For the point $R_1 = (0, 0)$ we obtain $a > 0$, and for $R_3 = (1, 1)$ we obtain $1 + 4 - 2(1 + a + 1) + a = 1 - a > 0$.

Finally, for $a > 1$, $R_2 = (1, 1)$ and substituting it in δ_{K_a} we obtain $1+4-2(1+a+1)+a = 1-a < 0$. For the point $R_1 = (0, 0)$ we obtain $a > 0$, and for $R_3 = (a, a)$ the result is $a^2 + 4a^2 - 2a(1 + a + a) + a = a^2 - a = a(a - 1) > 0$.

So, we deduce that R_2 is located in the interior of the ellipse δ_{K_a} while R_1 and R_3 are located outside the curve δ_{K_a} for any case. As this curve is in the boundary of different basins of attraction, the immediate basin of R_2 must be in the region delimited by δ_{K_a} which involves that $\mathcal{A}^*(R_2)$ is bounded. □

Let us observe that line $y = x$ divides the singular set δ_{K_a} in two symmetric parts, $\delta_{K_a} = \delta_{K,l} \cup \delta_{K,r}$ whose equations are:

$$\begin{aligned} \delta_{K,l} : x &= y - \sqrt{2y(1+a) - (3y^2 + a)}, \\ \delta_{K,r} : x &= y + \sqrt{2y(1+a) - (3y^2 + a)}. \end{aligned}$$

If we consider a small neighborhood U of the fixed point R_i that belongs to the prefocal line δ_{Q_i}, the points belonging to $U \cap Z_0$ have no preimages, while the points belonging to $U \cap Z_2$ have two distinct preimages given by an unbounded area $K_a^{-1}(U)$ that must include the line $y = y^*$. As it is shown in Figure 4, the fixed point $R_i = (x_i^*, x_i^*)$ is in the intersection of the two curves that form the boundary of Z_2, so the boundary of the disk, ∂U, cuts each of these curves in two different points. When ∂U cuts the curve $y = x$ their preimages go to $\pm\infty$ asymptotically to the line $y = y^*$ as function Δ does too. When ∂U cuts the prefocal line $x = x^*$ their preimages go to the focal points. So, the preimage of the disk U is formed by a bounded region, with the two focal points in its boundary, around the fixed point and by two unbounded regions that start from these focal points. In Figure 4, we observe two cases for $a < 0$; in the left figure the two focal points are inside Z_0 and in the right figure there is one focal point inside Z_2. The preimages of the boundary of the disk, $K_a^{-1}(\partial U)$, in this figure are the magenta and cyan curves; magenta curves correspond to the preimages of the upper side of the disk inside Z_2 and the cyan curves correspond to the bottom side. Let us notice that both preimages go to ∞ as the two side of the disk inside Z_2 cut the line $y = x$.

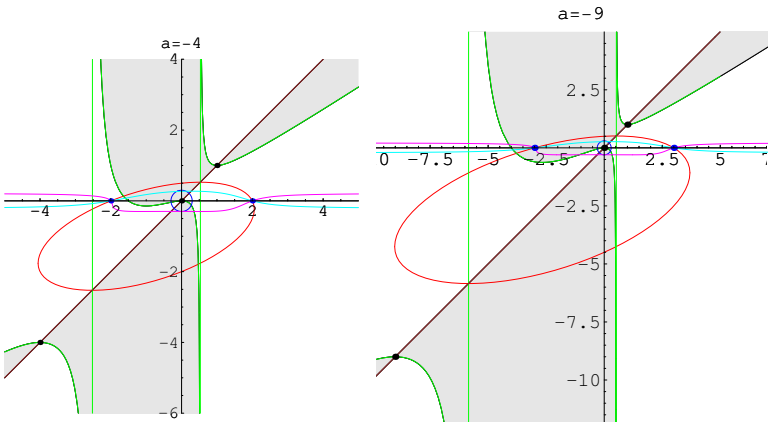

Figure 4. Sketch of the preimages $K_a^{-1}(U)$ of the neighborhood U of the fixed point that belongs to the prefocal line.

Nevertheless, let us notice that when one of the focal points is inside Z_2 the preimages of the border of the disk, $K_a^{-1}(\partial U)$, have three different pieces inside Z_2 and the preimages of one of them does not go to ∞ as it does not cut the line $y = x$; in fact, their preimages give the border of a disk, as you can see in the right picture of Figure 5.

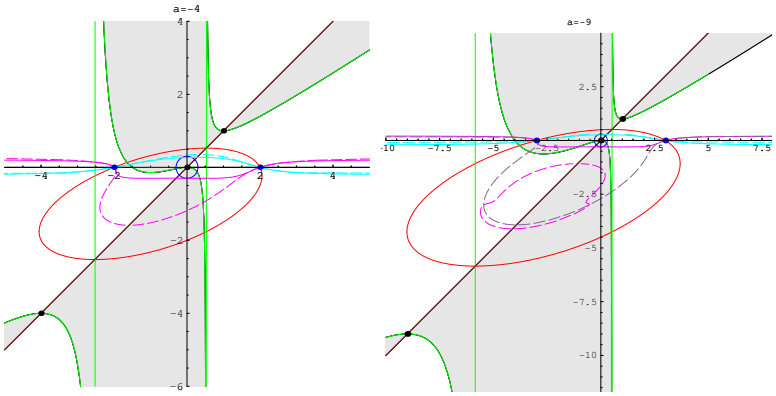

Figure 5. Sketch of the preimages $K_a^{-2}(U)$ of the neighborhood U of the fixed point that belongs to the prefocal line.

In the following, we obtain all types of curves in the set of non definition, Λ, of Kurchatov's map. We calculate the preimages of the arcs obtained from the intersection of the different curves with Z_2, starting from the curve δ_{K_a}. The different arcs are colored in blue in Figure 6, and their corresponding rank-1 preimages are colored in magenta.

Proposition 3.12. *Let γ be an arc defined by $\Gamma \bigcap Z_2$, where $\Gamma \in \Lambda = \bigcup_{n\geq 0} K_a^{-n}(\delta_{K_a})$ and let LC be the critical set defined in (3.3); then, γ satisfies one of the following statements:*

- *The arc γ goes from the curve LC to the line $y = x$.*
- *The arc γ connects the curve LC with the curve LC in different points.*
- *The arc γ connects the line $y = x$ with the line $y = x$ in different points.*

Moreover, if an arc cuts the line $y = x$, then its preimages go to infinity. If it does not cut the line $y = x$ its preimages give a closed curve.

Proof. . The intersection of the critical set δ_{K_a} with Z_2 gives two arcs, colored in blue in Figures 6(A) and 6(B) and denoted γ. In both cases, the intersection of the arc with ∂Z_2 is produced at two points: one on *LC* and the other on line $y = x$. Then, both arcs connect the curve *LC* and line $y = x$. Now, let us see how is the rank-1 preimage of such arcs.

Let us consider the preimages of the points of γ for the case (A), moving along γ from right to left. The preimages of the intersection of γ with line $y = x$ are infinity due to the term Δ in the map K_a^{-1} (see (3.2)). As $x > 0$, the second component of K_a^{-1} is positive. For each point of γ we have two preimages, starting at $+\infty$ and $-\infty$, respectively; when γ reaches the prefocal line, these two preimages are the focal points. The curve $K_a^{-1}(\gamma)$ turns at these points and crosses the invariant line $y = y^*$ and finally, the two preimages merge at the point corresponding to the preimage of the point of γ on the curve *LC*, when $y = x$.

We now consider the intersections of this curve with Z_2. We again obtain two arcs. One of them connects the curve LC and line $y = x$. If one prefocal point is inside Z_2, the other arc connects LC with LC, intersecting LC at two different points (see this type of arc colored in blue in Figure 6 (C)).

Let P and P' be the intersection points of γ with LC; the preimages of this type of curve γ form a closed curve $K_a^{-1}(\gamma)$ since the two preimages of these curve coincide at the points $K_a^{-1}(P)$ and $K_a^{-1}(P')$, as we have obtained previously.

If we now consider the intersection of this closed curve with Z_2, we obtain an arc that cuts the line $y = x$ at two different points. We represent this type of arc in blue in Figure 6(D).

As seen before, the preimages of each point on line $y = x$ are $\pm\infty$, due to the function Δ. As the arc γ does not cut the curve LC, their preimages do not coincide at any point. The preimage of such arc can be seen colored in magenta in Figure 6(D). If this curve is located in Z_0, then it has no preimages.

So, three types of arcs are obtained: arcs connecting LC with LC, arcs connecting LC with line $y = x$ and arcs connecting line $y = x$ with line $y = x$.

In a similar way, it can be described the curves preimages of the arc γ in Figure 6(B) obtaining the same type of arcs, and so, the same type of curves. □

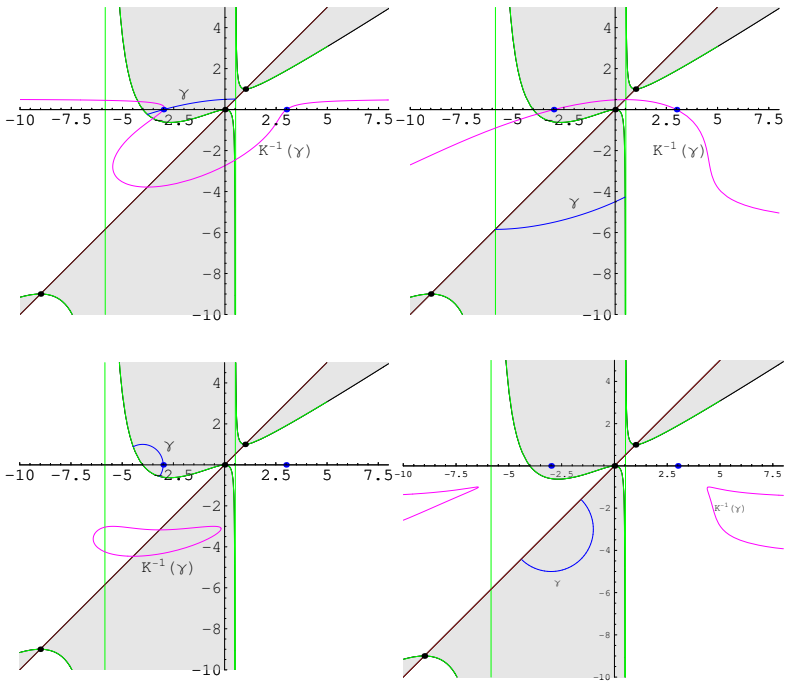

Figure 6. Sketch of the preimages $K^{-1}(\gamma)$ of different curves embedded in Z_2.

Due to the classification obtained above, we have the description of the curves $\Gamma \in \Lambda$: they go from $-\infty$ to $+\infty$, passing through the focal points, they form closed curves or they form tongues.

3.4. Dynamical planes

Following the results of the previous section, it is possible to make an outline of dynamical planes depending on whether there is a focal point inside Z_2 or the two focal points are in Z_0.

To describe the basin boundaries we have to consider the singular set δ_{K_a} and its preimages. From Figure 3 it is observed that $\delta_{K_a} \cap Z_2$ is divided into two different branches denoted by $\delta_{K,b}$ and $\delta_{K,t}$ such that $\delta_{K_a} \cap Z_2 = \delta_{K,b} \cup \delta_{K,t}$. Moreover, it can be checked that $\delta_{K,b} \subset \delta_{K,r}$ and $\delta_{K,t} \subset \delta_{K,l}$. The portion of δ_{K_a} located into Z_0 has no preimages whereas the portion located into Z_2 is made up of two disjoint branches, each one having two rank-1 preimages. Therefore, $K_a^{-1}(\delta_{K_a})$ is made up of four branches. As Lemma 3.8 tell us, one of the focal points can belong to $\delta_{K,b} \cup \delta_{K,t}$ or none of them are in these branches.

In Figure 7 we have drawn the preimages $K_a^{-1}(\delta_{K_a})$ and $K_a^{-2}(\delta_{K_a})$ for two different cases: the first one corresponds to the case where none of the focal points are in Z_2 and the second case corresponds to one focal point in Z_2. Let us observe that all the preimages of δ_{K_a} go from $-\infty$ to $+\infty$ turning at the focal points if the two focal points are in Z_0. However, we can observe the emergence of closed curves that do not cross the focal points when one focal point is in Z_2, as it was predicted in Proposition 3.12. The two points where this curve is cut by other preimage of δ_{K_a} correspond to the two preimages of the focal point.

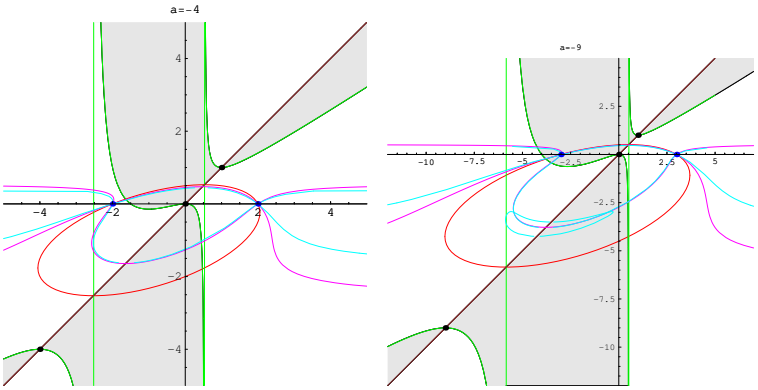

Figure 7. Sketch of the preimages $K_a^{-1}(\delta_{K_a})$ and $K_a^{-2}(\delta_{K_a})$ for $a = -4$ and $a = -9$.

The corresponding dynamical planes can be observed in Figure 8: in the left figure, the two focal points are embedded in Z_0, in the right one, there is a focal point in Z_2.

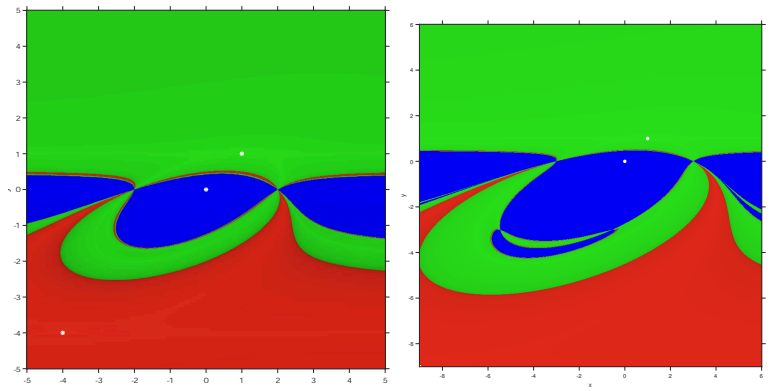

Figure 8. Dynamical planes for $a = -4$ and $a = -9$.

3.5. *Bifurcations*

In this section, we study three types of bifurcation: when the number of fixed and focal points change, the changes produced when the number of the preimages of focal points changes and the changes produced in the dynamical system when bounded and isolated preimages of some basins of attraction appear.

The design of the basins of attraction changes depending on the number of preimages of the focal points. So, we study what happens when one focal point has not any preimage and the other has only one preimage. As Lemma 3.8 states, the values of the parameter for which Q_1 has one preimage are: $a = -3 - 2\sqrt{2}$, $a = \frac{1}{2}(2 + \sqrt{2}$ and $a = 2(2 - \sqrt{2})$. For $a = -3 + 2\sqrt{2}$, $a = \frac{1}{2}(2 - \sqrt{2})$ or $a = 2(2 + \sqrt{2})$, Q_2 has one preimage.

If focal points have not preimages, the pieces of δ_{K_a} and their preimages embedded in Z_2 go from line $y = x$ to the rational function o vice versa as they cut the prefocal line and have to cross the focal points. So, if these preimages of δ_{K_a} also go from line $y = x$ to the rational function o vice versa, all the borders of the basins of attraction of the fixed points go across the focal points similarly to those drawn in Figure 7(A) and their dynamical plane are similar to Figure 8(A) with the pieces of the basins of attraction going to the focal points.

However, if one focal point has two preimages, then the preimages of δ_{K_a} include closed and bounded curves that do not cut the focal points as they can go to the preimages of them, as it can be seen in Figure 7(B) and their dynamical plane are similar to Figure 8(B). In the following we consider the bifurcation case corresponding to one focal point with one preimage. As we can see in Figure 9(A), the preimages of δ_{K_a} include closed and bounded curves that are tangent among themselves in the preimages of the focal point.

In Figure 9(A) the curve δ_{K_a} is colored in red, $K^{-1}(\delta_{K_a})$ in magenta, $K^{-2}(\delta_{K_a})$ in cyan and $K^{-3}(\delta_{K_a})$ is dashed and colored in blue. The corresponding dynamical plane can be seen in Figure 9(B).

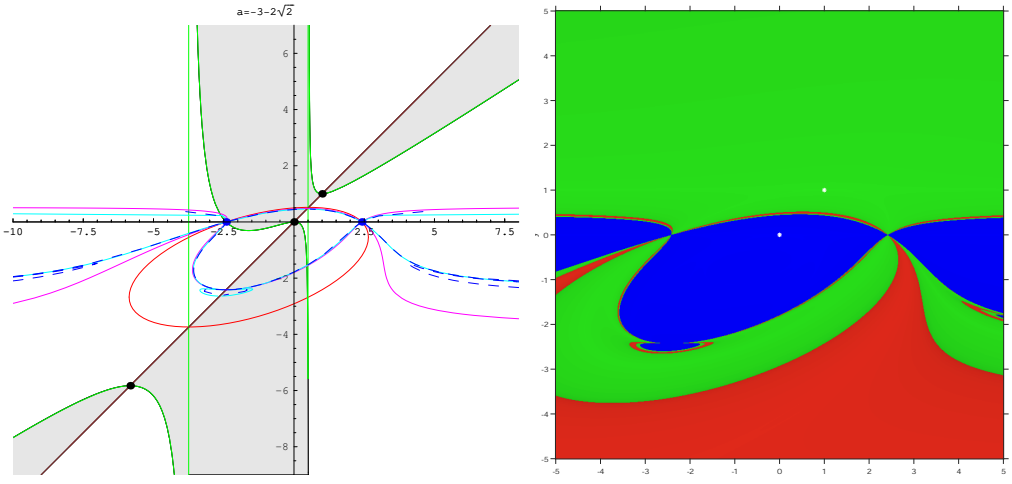

Figure 9. Sketch of the preimages and dynamical plane for $a = -3 - 2\sqrt{2}$.

Additionally, if a is closed enough to one of these bifurcation values the preimages of δ_{K_a} include closed and bounded curves isolated inside $K^{-1}(\delta_{K_a})$, (see Figure 10(A)) that give rise to bounded and isolated regions in the dynamical plane (see Figure 10(B)).

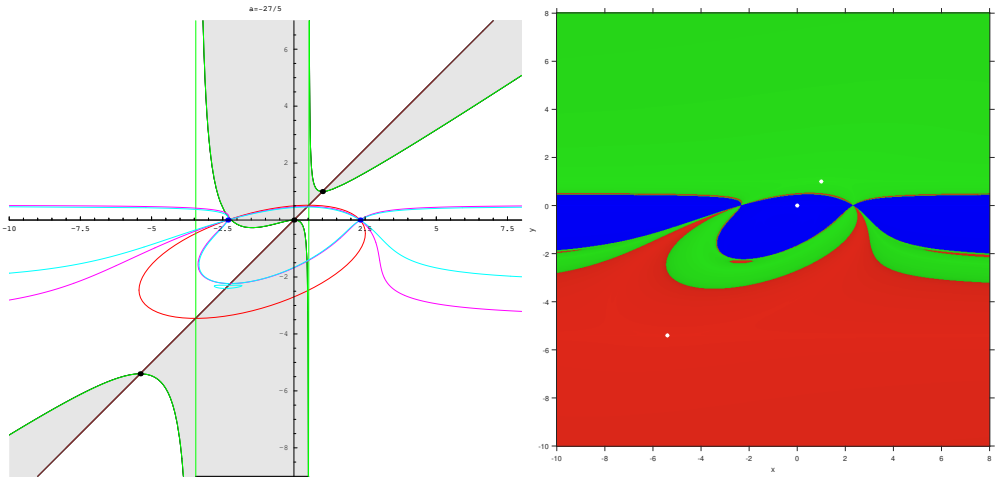

Figure 10. Sketch of the preimages and dynamical plane for $a = -27/5$.

These bounded curves approach each other until they are tangent at the bifurcation point. After this point, the curves drift apart until the bounded and isolated curves disappear. This type of bifurcation corresponds to the values of the parameter where $K^{-1}(\delta_{K_a})$ is tangent to the rational function LC.

Finally, for $a = 0$ and $a = 1$ two fixed points collapse together with the focal points in the bifurcation points; in these cases all the borders pass through the fixed point, that is also a focal point (see Figures 11 and 12).

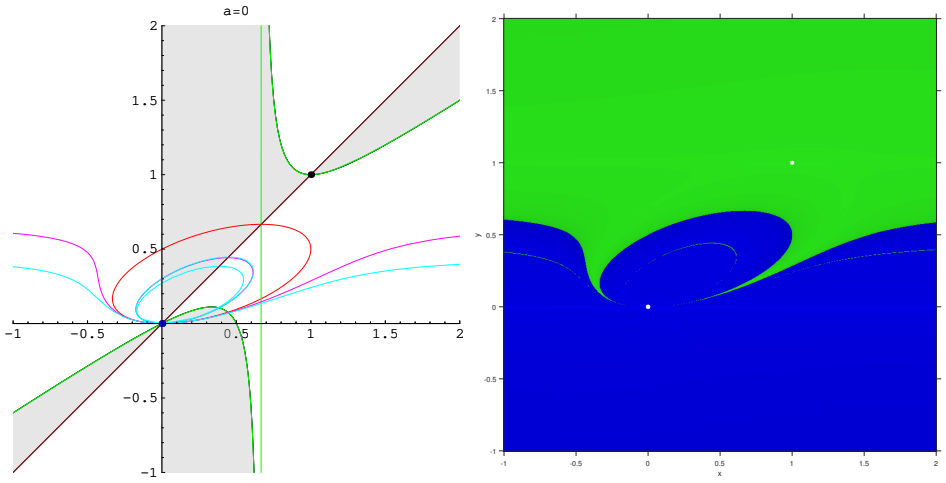

Figure 11. Sketch of the preimages and dynamical plane for $a = 0$.

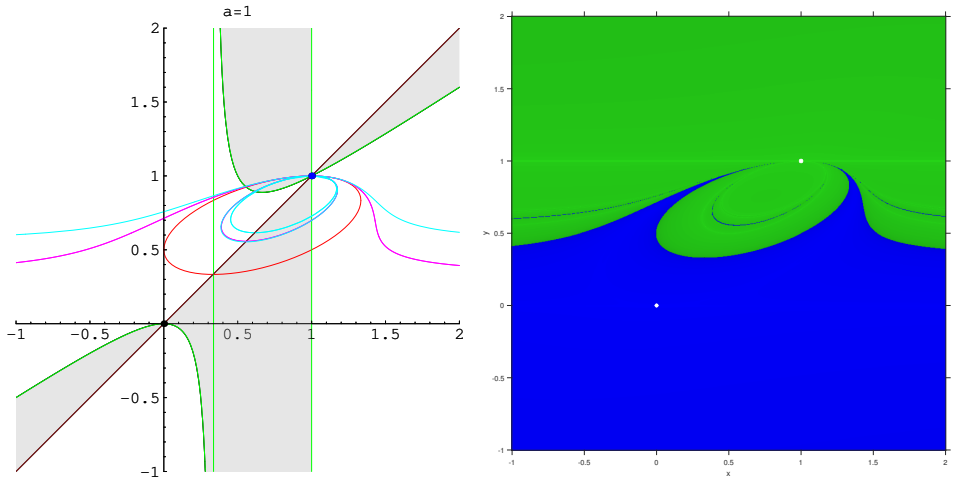

Figure 12. Sketch of the preimages and dynamical plane for $a = 1$.

Nevertheless, if we consider a small interval around $a = 0$ or $a = 1$, we observe that there are three attractive fixed points and two focal points and only one of the focal points have two preimages; so, the dynamics of the map does not change in a narrow interval of these bifurcations points, as we can observe in Figure 13.

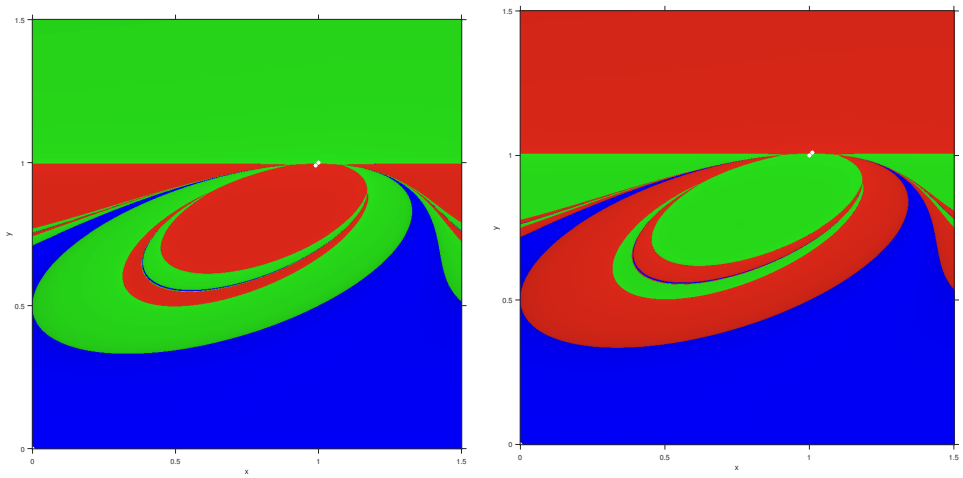

Figure 13. Dynamical planes for $a = 0.99$ and $a = 1.01$.

If one focal point is in the boundary of Z_2, then it has one preimage. The dynamical plane is similar to the first case: there appear bounded and unbounded areas that do not have the focal points as limits and belong to the basins of attraction of all the fixed points. The difference is that bounded areas touch the immediate basin of R_2 at a point which is the preimage of the focal point. The dynamical plane is similar to that of $a = -3 - 2\sqrt{2}$, (see Figure 9).

Therefore, all the possible performance of the Kurchatov method on a generic cubic polynomial is explained. We can summarize these results in the line of parameters shown in Figure 14, obtaining a bifurcation diagram where each color represents one type of dynamical plane: cyan corresponds to the first type, violet to the second one and magenta to the last type. The cases $a = 0$ and $a = 1$ correspond to dynamical planes where the focal points are not simple and have been studied separately.

Figure 14. Parameter line.

4. Conclusions

A complete description of the dynamical planes for every value of the parameter has been carried out. In fact, we have obtain three different types of dynamical planes:

1. If one focal point is inside Z_2, then it has two preimages. There appear bounded areas that do not have the focal points as limits and belong to the basins of attraction of all the fixed points. The bounded areas touch the immediate basin of R_2 at two points (which are the preimages of the focal point). The unbounded areas have the focal points as limits.
2. If the focal points are inside Z_0, but they are closed enough to the boundary of Z_2, the bounded areas belonging to the basins of attraction of the fixed points still remain but they do not touch the immediate basin of R_2. Moreover, there exist unbounded areas that do not reach the focal points.
3. Finally, when the focal points are inside Z_0 and not close to Z_2, the bounded areas have disappear and all the areas are unbounded and have focal points as limits.

We have represented these different dynamical behaviours for every value of the parameter in a bifurcation diagram, the parameter line.

Along this paper we have shown that this iterative scheme is completely stable for any polynomial of degree three, since the only attractors that appear for any value of the parameter are the roots of the polynomial.

Acknowledgments

This paper is supported by the MCIU grant PGC2018-095896-B-C22. The first and the last authors are also supported by University Jaume I grant UJI-B2019-18. Moreover, the authors would like to thank the anonymous reviewers for their comments and suggestions.

Conflict of interest

All authors declare no conflicts of interest in this paper.

References

1. V. A. Kurchatov, On a method of linear interpolation for the solution of funcional equations (Russian), *Dolk. Akad. Nauk SSSR*, **198** (1971), 524–526. Translation in *Soviet Math. Dolk.* **12**, 835–838.
2. M. Petković, B. Neta, L. Petković, J. Džunić, *Multipoint Methods for Solving Nonlinear Equations*, Boston: Academic Press, 2013.
3. A. Cordero, T. Lotfi, P. Bakhtiari, J. R. Torregrosa, An efficient two-parametric family with memory for nonlinear equations, *Numer. Algorithms*, **68** (2015), 323–335. https://doi.org/10.1016/j.worlddev.2014.11.009
4. A. Cordero, T. Lotfi, J. R. Torregrosa, P. Assari, S. Taher-Khani, Some new bi-accelerator two-point method for solving nonlinear equations, *J. Comput. Appl. Math.*, **35** (2016), 251–267. https://doi.org/10.1002/sim.6628
5. X. Wang, T. Zhang, Y. Qin, Efficient two-step derivative-free iterative methods with memory and their dynamics, *Int. J. Comput. Math.*, **93** (2016), 1423–1446. https://doi.org/10.1080/00207160.2015.1056168
6. P. Bakhtiari, A. Cordero, T. Lotfi, K. Mahdiani, J. R. Torregrosa, Widening basins of attraction of optimal iterative methods for solving nonlinear equations, *Nonlinear Dynam.*, **87** (2017), 913–938. https://doi.org/10.1007/s11071-016-3089-2
7. C. L. Howk, J. L. Hueso, E. Martínez, C. Teruel, A class of efficient high-order iterative methods with memory for nonlinear equations and their dynamics, *Math. Meth. Appl. Sci.*, **41** (2018), 7263–7282. https://doi.org/10.1002/mma.4821
8. B. Campos, A. Cordero, J. R. Torregrosa, P. Vindel, A multidimensional dynamical approach to iterative methods with memory, *Appl. Math. Comput.*, **271** (2015), 701–715. https://doi.org/10.1016/j.amc.2015.09.056
9. B. Campos, A. Cordero, J. R. Torregrosa, P. Vindel, Stability of King's family of iterative methods with memory, *Comput. Appl. Math.*, **318** (2017), 504–514. https://doi.org/10.1016/j.cam.2016.01.035
10. N. Choubey, A. Cordero, J. P. Jaiswal, J. R. Torregrosa, Dynamical techniques for analyzing iterative schemes with memory, *Complexity*, **2018** (2018), Article ID 1232341, 13 pages.
11. F. I. Chicharro, A. Cordero, N. Garrido, J. R. Torregrosa, Stability and applicability of iterative methods with memory, *J. Math. Chem.*, **57** (2019), 1282–1300. https://doi.org/10.1007/s10910-018-0952-z
12. F. I. Chicharro, A. Cordero, N. Garrido, J. R. Torregrosa, On the choice of the best members of the Kim family and the improvement of its convergence, *Math. Meth. Appl. Sci.*, **43** (2020), 8051–8066. https://doi.org/10.1002/mma.6014
13. F. I. Chicharro, A. Cordero, N. Garrido, J. R. Torregrosa, Impact on stability by the use of memory in Traub-type schemes, *Mathematics*, **8** (2020), 274.
14. A. Cordero, F. Soleymani, J. R. Torregrosa, F. K. Haghani, A family of Kurchatov-type methods and its stability, *Appl. Math. Comput.*, **294** (2017), 264–279. https://doi.org/10.1016/j.amc.2016.09.021

15. R. C. Robinson, *An Introduction to Dynamical Systems, Continous and Discrete*, Providence: Americal Mathematical Society, 2012.

16. G. Bischi, L. Gardini, C. Mira, Plane maps with denomiator I. Some generic properties, *Int. J. Bifurcations Chaos*, **9** (1999), 119–153. https://doi.org/10.2307/605565

17. G. Bischi, L. Gardini, C. Mira, Plane maps with denomiator II. Non invertible maps with simple focal points, *Int. J. Bifurcations Chaos*, **13** (2003), 2253–2277. https://doi.org/10.1142/S021812740300793X

18. G. Bischi, L. Gardini, C. Mira, Plane maps with denomiator III. Non simple focal points and related bifurcations, *Int. J. Bifurcations Chaos*, **15** (2005), 451–496. https://doi.org/10.1142/S0218127405012314

19. G. Bischi, L. Gardini, C. Mira, New phenomena related to the presence of focal points in two dimensional maps, *J. Ann. Math. Salesiane*, (special issue Proceedings ECIT98), **13** (1999), 81–90.

20. A. Garijo, X. Jarque, Global dynamics of the real secant method, *Nonlinearity*, **32** (2019), 4557–4578. https://doi.org/10.1088/1361-6544/ab2f55

21. A. Garijo, X. Jarque, The secant map applied to a real polynomial with multiple roots, *Discrete Cont. Dyn-A.*, **40** (2020), 6783–6794. https://doi.org/10.3934/dcds.2020133

22. L. Gardini, G. Bischi, D. Fournier-Prunaret, Basin boundaries and focal points in a map coming from Bairstow's method, *Chaos*, **9** (1999), 367–380.

23. M. R. Ferchichi, I. Djellit, On some properties of focal points, *Discrete Dyn. Nat. Soc.*, **2009** (2009), Article ID 646258, 11 pages.

24. G. Bischi, L. Gardini, C. Mira, Contact bifurcations related to critical sets and focal points in iterated maps of the plane, *Proceedings of the International Workshop Future Directions in Difference Equations*, (2011), 15–50.

25. N. Pecora, F. Tramontana, Maps with vanishing denominator and their applications, *Front. Appl. Math. Stat.*, **2** (2016), 12 pages.

AIMS Press